Mathematical Modelling and Analysis. Ed. A.Buikis
Volume 12 Number 1, 2007, pages 121–130
 ISSN 1392-6292 print, ISSN 1648-3510 online

GENERATING OF REFORMAT SLICES IN NEURAL AND CARDIO-TOMOGRAPHY

L. MOCKUS[1], M. MEILŪNAS[1], M. PAULINAS[1], A. UŠINSKAS[1] and D. ZAKARKAITĖ[2]

[1] *Vilnius Gediminas Technical University*

Sauletėkio av. 11-L424B, LT-10223 Vilnius, Lithuania

[2] *Clinic of Heart Diseases, Vilnius University*

Santariškių Str. 2 LT-08661 Vilnius, Lithuania

E-mail: mm@fm.vtu.lt; andrius.usinskas@el.vtu.lt

Received October 1, 2006; revised November 1, 2006; published online March 1, 2006

Abstract. A lot of medical diagnostics problems are related to the reconstruction of three dimension (3D) images from the cross sections of the regions of interest. Such reconstructions are very desirable for evaluation of disease or planning of surgical treatment.

This paper reviews recent 3D preprocessing work of authors in human brain blood vessels structure recognition and localization of aneurysms as well as analysis of the right ventricular of the human heart. Here we present some approximation techniques for generation of reformatted images.

Key words: reformat slices, reformat contours, MRI

1. Introduction

An important task in medical diagnostics is generation of extra data from the observations. These data is often urgent in the analysis of neural and cardio-tomography. In this paper two problems in generating of the extra slices are considered: computation of reformat slices in MRI tomography of human intracranial blood vessels [6] and computation of reformat slices of right ventricle surface from three orthogonal contours [7].

There are several techniques of generating the reformat slices. Interpolation methods were used in [2]. A novel approximation algorithm of producing extra slices from observation data by using the resize technique is proposed in this paper. This very well-known technique in signal processing and analysis field was applied for generating the extra slices in MRI images. The developed simple and fast algorithm is based on using the open source library "ImageMagick". Reconstruction of the right ventricle's surface is realized by

transforming three given orthogonal contours. The proposed transformation is easy to implement in an ordinary personal computer.

In this paper we describe medical images and MRI slices, which are in DICOM format, as a matrix $[f]$:

$$[f] = \{f_{i,j} : i = 1, \ldots, M; j = 1, \ldots, N\},$$

where $f_{i,j}$ represents the value of the image function in the ith row and jth column, M is the number of rows and N is the number of columns [4].

2. Equalization of Spacing of MRI Volume Data

Analysis of volumetric information in the set of medical images is a very important area of medical data processing in this decade. It become possible to compute various parameters of 3D objects by using ordinary computers. One of such objective is to analyse magnetic resonance imaging (MRI) slices and recognise vessels regions in such images. The information about vessels characteristics could be used for the detection of aneurysm region and calculation of important parameters for a possible surgery treatment.

Before analysis of all slices like one unit the equalization of spacing of MRI volume data must be done. Usually the MRI slices have the one pixel spacing in horizontal (image) plane and another spacing in vertical (set of images) plane. For example, after examination of the head vessels there could be produced 72 slices with 1 mm slice thickness. Such slices could present the matrix of pixels with 1024 rows and 768 columns. Five pixels could correspond to 1 mm (pixel spacing was 0.1953). In this case the neighbour pixel in horizontal plane will be in 0.2 mm and the neighbour pixel in vertical place in 1 mm. So pixel spacing in horizontal and vertical directions differs 5 times.

Equalization of spacing of MRI volume data could be achieved in several ways. One of them is to reduce the size of slices and increase the number of such slices. Appendage of extra slices will not add more information, but will let to understand information about vessels and aneurysm region in a better way. The extra slices could be a product of adjacent slices. In this case the filter as the last operation of resize function plays the crucial role for defining quality of produced slices. Thus our task is to evaluate available filters and select the best filter for producing extra slices for vessels and aneurysm analysis in MRI images.

The impact of such filtering is illustrated in the next case. The 90 slices 512×384 of MRI images of human brain were used as input data. After resize operation of 3D array (a set of all MRI slices) in vertical plane the 360 reformat slices were produced. The expectation that each fourth reformat slice must be the same as like input slice is wrong. The image of 20th MRI slice (Fig. 1*a*), reformat image after applying the Gaussian filter on such slice (Fig. 1*b*) and visualised difference between reformat and original images (Fig. 1*c*) are shown in Fig. 1. Such difference was calculated as image of absolute value of difference between reformat B and original A images:

$$C_{m,n} = \sum_{m=1}^{M} \sum_{n=1}^{N} | B_{m,n} - A_{m,n} |,$$

where m, n was the row and column numbers respectively, $m = 1, 2, \ldots, M$; $n = 1, 2, \ldots, N$ ($M = 512$ was the number of rows and $N = 384$ was the number of columns).

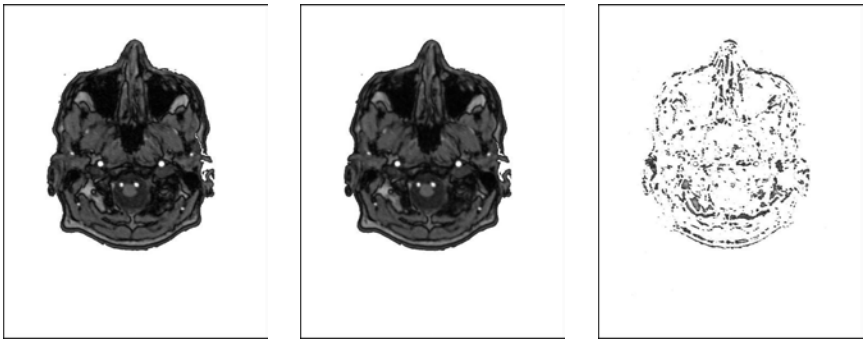

a) b) c)

Figure 1. Impact of the filtering on MRI slice (a – original image of slice, b – reformat image of such slice after applying Gaussian filter, c – visualised difference between reformat and original images).

The range of the difference image (Fig. 1*c*) was 40, and the maximum value of the brightness of original image was 255. The original image was $40/255 \times 100 \approx 16$ % distorted by using digital filtering technique. So, there is a need to measure fitting of original and respectively reformat images E ("match criterion"). We chose the following expression for E:

$$E = \sum_{l=1}^{L} \left(\hat{A}^l - \hat{B}^l \right)^2,$$

where l is the slice number, $l = 1, 2, \ldots, L$ ($L = 90$ is the number of slices in MRI experiments); $\hat{A}, \hat{B}$ are averages of brightness of image A and image B respectively.

However, in addition there is a need of the "smoothness criterion" of all reformat images to ensure smooth pass of brightness at adjacent reformat slices J [5]. We introduce them in the following form:

$$J = \sum_{l=2}^{L-1} \left(\frac{\hat{B}^{l-1} - 2\hat{B}^l + \hat{B}^{l+1}}{h^2} \right)^2 h, \tag{2.1}$$

where h is the distance between adjacent slices. The expression in the brackets of (2.1) is an approximation of the second derivative in vertical direction.

The final criterion K for selection of the best filter for MRI slices reformat operation was taken as follows:

$$K = wJ + (1 - w)E, \tag{2.2}$$

where w is the weight parameter. K contains information on the match between original and reformat slices (term E) and on smoothness of the obtained reformat slices (term J). Such expressions is often used for a curve and surface fitting [5]. We use (2.2) as a quality criterion for generated extra data set.

Fourteen filters of library "ImageMagick" (Bessel, Blackman, Box, Catrom, Cubic, Gaussian, Hanning, Hermite, Lanczos, Mitchell, Point, Quadratic, Sinc, Triangle) were used to determine the best filter for MRI images. Our main problem in this step was to select the best filter from this library, so we modified slightly the final criteria by normalising the corresponding terms as follows:

$$\hat{K} = w\frac{J}{J_{max}} + (1 - w)\frac{E}{E_{max}}, \tag{2.3}$$

where E_{max} and J_{max} are maximal value of criteria in the set of filter mentioned above.

3. Filters

While resizing images, there must be incorporated or eliminated additional samples using interpolation or other methods of approximation. Various techniques were used for this task, one of them is the digital low-pass filtering.

In digital signal processing, a digital filter is any electronic filter that works by performing digital mathematical operations on an intermediate form of a signal. Digital filters can achieve virtually any filtering effect that can be expressed as a mathematical algorithm [1].

Filters are applied using the convolution of signal function $f(t)$ and filter kernel $h(t)$. In two dimensional case of discrete argument function the convolution is defined as:

$$c[m] = f[m] \otimes h[m] = \sum_{j=0}^{J-1} h[j]f[m - j],$$

where J characterises the dimension of sliding window.

In the case of digital image and separable filter kernels, image rows are convolved with kernel and intermediate picture is obtained, next the same convolution is performed on all intermediate image columns and final result is produced [1].

All experiments were conducted using ImageMagick library image resampling facilities and all built-in filters were tested. Most of the used filters are finite impulse response (FIR), however, Bessel, Gaussian and Sinc are infinite impulse response filters (IIR). Bessel and Sinc are windowed (brought down to zero) with Blackman filter.

The simplest used filters were the point and box filters. They are simplest nearest adjacent interpolation. The box filter simply computes the average of

the selected size window. Another filter was Gaussian, which is popular due to its many convenient analytical properties, such as positivity and its own Fourier transform [3].

In all experiments the Blackman kernel performed well. It is defined as:

$$h(t) = 0.42 + 0.5\cos\left(\frac{2\pi n}{N-1}\right) + 0.08\cos\left(\frac{4\pi n}{N-1}\right).$$

This window was developed in search for an ideal window. It is similar to Gaussian window in shape, but it has a better attenuation at stop frequency.

Also, the Lanczos-windowed Sinc function was tested. Sinc filter is an idealised filter that removes all frequency components above a given bandwidth and leaves the low frequencies alone. It is shaped like a rectangular function in the frequency domain and like a Sinc function in the time domain. Realistic filters can only approximate this. This function has been shown as particularly useful for graphics applications [8]. The two-lobed Lanczos-windowed Sinc function is defined as [3]:

$$f(x) = \frac{\sin(\pi x)\sin(2\pi x)}{2\pi^2 x^2}, \quad |x| < 2.$$

4. Experiment

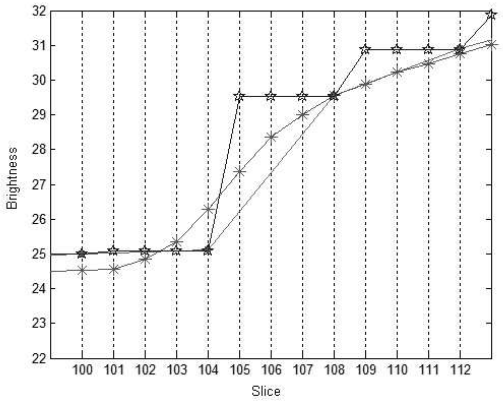

Figure 2. Average of smoothness criterion (circles denote original slices, asterisks denote Gaussian filtering, stars denote Box filtering).

The 14 filters of ImageMagick library were investigated. Fig. 2 shows distribution of average of smoothness criterion (2.1) of original images and after applying Gaussian and Box filters (Fig. 2). Value of brightness average increases in discreet manner – slices 100, 104, 108, and 112 correspond to

original slices 25, 26, 27, and 28. For computing extra slices between these original slices the digital filtering technique was used. The Gaussian filter produces extra slices in smoother way, but 3 of 4 original slices were changed (for example, the average of brightness of slice 104 did not correspond to the average of brightness of slice 26). However the Box filter produced exactly the same original slices, but extra slices were discreet: the change of average of brightness was the same as in adjacent original images. So the two criteria were needed to evaluate the smoothness of extra slices and to estimate how the produced slices match the original slices. In the ideal case the difference between adjacent slices must be equally distributed (like Gaussian filtering) and the original slices must be unchanged (like Box filtering).

Fig. 3*a* shows the distribution of average via all 90 slices of MRI angiography in the vessel region. Usually such dependence has a lot variations and several peaks. Thus it is important to produce extra slices that the properties of vessels will stay the same. The Fig. 3*b* shows impact of Gaussian filtering and 3*c* – of Box filtering. Such filtering was done after producing 4 times more slices (90 slices became 360 slices). It is clear that information about vessels region is more useful to preserve with smoothest filter like Gaussian in this case.

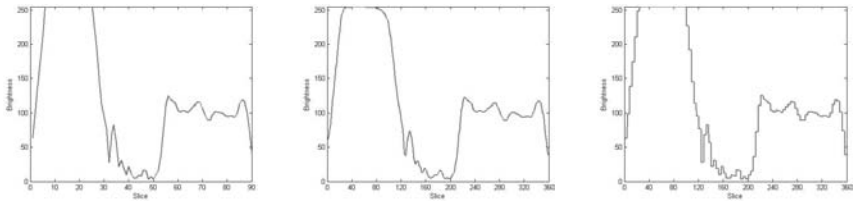

a) b) c)

Figure 3. Impact of filtering the vessel region in the set of MRI scans: a) the original image, b) Gaussian image, c) Box image).

The values of the normalized criteria J and E are presented in Table 1. The choice of w depends on the problem to be solved. In our case it was the evaluation of numerical characteristics of aneurysms. Thus it is necessary to select w values by analysing a wide range of situations in the physical model of blood vessel networks in order to meet this aim. We used artificial network based on silicon vessels. Performed investigation shows acceptable values of w in interval $(0.85, 0.95)$.

The largest smoothness was achieved by the smallest values 0.302 (Sinc filter) and 0.305 (Lanczos filter). The largest roughness is shown by Box, Point (1.000) and Blackman (1.000) filters. However the criterion of match is conversely distributed. The maximum mismatch achieved by Lanczos (1.000) and Sinc (0.978) filters, the exact match is achieved by Box and Point filters (0) and Blackman filter (0.449). It seems that in filtering MRI angiography images there was no difference between Box and Point filters.

Table 1. Normalized values of the used criteria.

Filter	J/J_{max}	E/E_{max}
Bessel	0.310	0.921
Blackman	0.435	0.449
Box	1.000	0.000
Catrom	0.308	0.910
Cubic	0.323	0.921
Gaussian	0.320	0.876
Hanning	0.383	0.618
Hermite	0.380	0.640
Lanczos	0.305	1.000
Mitchell	0.309	0.899
Point	1.000	0.000
Quadratic	0.317	0.888
Sinc	0.302	0.978
Triangle	0.344	0.798

5. Reformat Contours Reconstruction of the Right Ventricle of a Human Heart

Main diagnostic methods in cardiology are ultrasound research and computed tomography (CT). For elaboration of algorithms CT images are used as the primary source of information.

The main purpose of this investigation is 3D reconstruction of the right ventricle's surface from three orthogonal sections in CT images. The initial data example is shown in Fig. 4*a*. These contours represent the right ventricle's volume. But it is a poor data for volume calculations. So, the original method for volume reconstruction is developed and presented in this paper.

Let we have three orthogonal contours F, G and H (see Fig. 4*a*). Let F be the main contour which can be deformed. We consider the other two orthogonal contours G and H as directing contours. The contour G helps to transform y coordinates of all points on the contour F and the contour H helps to transform x coordinates of point M (Fig. 4*a*). F and G crosses at points $A\,(x_A, y_A, z_F)$ and $B\,(x_B, y_B, z_F)$. After each transformation steps A and B are recalculated into A' and B'. Let us denote transformation of the main contour in z direction:

$$A\,(x_A, y_A, z_F) \rightarrow A'\,(x_{A'}, y_{A'}, z_F + \Delta z)\,,$$

$$B\,(x_B, y_B, z_F) \rightarrow B'\,(x_{B'}, y_{B'}, z_F + \Delta z)\,,$$

where $A'\,(x_{A'}, y_{A'}, z_F + \Delta z)$ and $B'\,(x_{B'}, y_{B'}, z_F + \Delta z)$ are positions of points A and B after transformation, Δz is the change in z coordination, it is used as the parameter of this numerical algorithm. We note that z can be both positive and negative.

Let us consider a transformation of all points on the contour F with the help of the contour G. The y coordinate of any point M can be expressed in

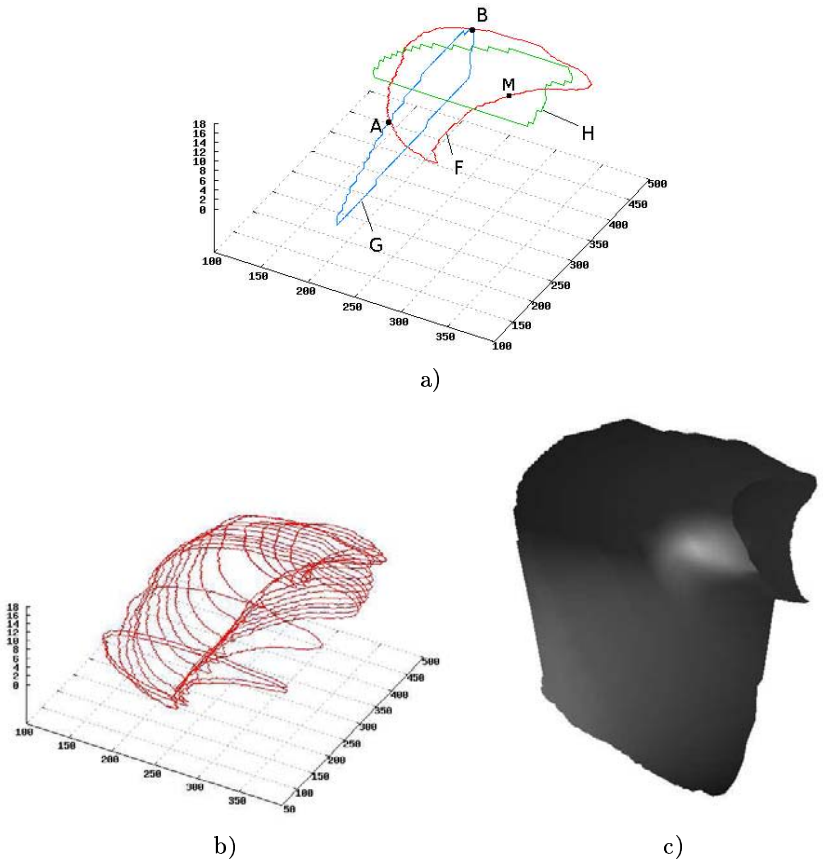

Figure 4. Right ventricle: a) three contours, b) some reformat contours, c) reconstructed surface.

the following way:

$$y_M = (1-t)\, y_A + t y_B. \tag{5.1}$$

Then the change of y value in the reformat contour is defined as:

$$\Delta y_M = (1-t)\, \Delta y_A + t \Delta y_B. \tag{5.2}$$

The new value of y coordinate is given by

$$y'_M = y_M + \Delta y_M, \tag{5.3}$$

where

$$y_M = y_A + t\,(y_B - y_A)\,, \quad t = \frac{y_M - y_A}{y_B - y_A}.$$

The formulas (5.2) and (5.3) are used for the calculation of y coordinate of the main contour's each point. The set of eight reformat contours in positive and negative z directions is shown in Fig. 4*b*. The case of x coordinate

transformation is not considered because it's analogous to y coordinate transformation.

All reformat contours have the same number of points, so the surface can be easily reconstructed (Fig. 4*c*). This is done by using the open source Mesa 3D graphics library [10]. The smallest surface element is triangle. Vertices of triangles are on two adjacent (reformat) contours (Fig. 5). One strip of linked triangles is constructed from each pair of reformat contours.

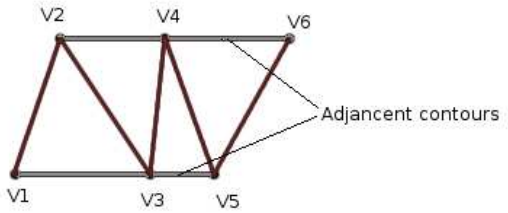

Figure 5. Strip of triangles with vertices.

The surface of the heart's right ventricle was successfully reconstructed from three orthogonal contours. It is necessary to remark that solution of this problem is the initial step of much more complicated volume estimation task from ultrasound images in real time scale. The achieved results will be used in the future research of ventricle's volume dynamics in time and for determination of heart's state.

6. Conclusions

Conclusions for pixel spacing algorithm for MRI angiography applications are as follows:

- The image resizing algorithm allows equalization of pixel spacing.
- The quality of reformat images depends on the used low-pass filter.
- The Box and Point filters produce the same results in MRI images.
- Mismatch between reformat and original slices is conditioned by smoothing property of the used filter.
- The convenient range of weight coefficient for evaluation filtered images is from 0.85 to 0.95.
- As a suitable filter for pixel spacing homogenisation in MRI can be recommended the Sinc and Lanczos filters.

Conclusions for reconstruction of the right ventricle are as follows:

- Ventricle representation with tree orthogonal contours requires extra lengths, angles, etc. for estimation of the volume, therefore reconstruction of the ventricle surface is needed.

- The surface of a human heart's right ventricle can be reconstructed from three orthogonal contours by transforming one contour with the help of the other two.
- The reconstructed surface can be used as a basis for further investigations, especially for the monitoring and control of the right ventricle volume dynamics in the time domain.

Acknowledgement

This investigation was supported by pan-European network for market-oriented, industrial R&D EUREKA Programme (EUREKA project E!3475 AMRA), and Lithuanian State Science and Studies Foundation (contract No. V-83/2006).

References

[1] A. Antoniou. *Digital Filters: Analysis, Design, and Applications.* McGraw-Hill Companies, New York, 1993.

[2] G. Chen, B. Miao, Y. Xie and S. Bao. Interpolation of 3D medical images in direction of slice thickness. *Medical Imaging and Information Sciences*, **20**(1), 34–39, 2003.

[3] Andrew S. Glassner. *Graphics gems I.* Morgan Kaufmann, San Francisco, 1990.

[4] Ernest L. Hall. *Computer Image Processing and Recognition.* Academic Press, 1979.

[5] P. Lancaster and K. Šalkauskas. *Curve and Surface Fitting: An Introduction.* Academic Press, 1986.

[6] A. Ronkainen, M. Puranen, J. Hernesniemi, R. Vanninen, P. Partanen, J. Saari, P. Vainio and M. Ryynanen. Intracranial aneurysms: MR angiographic screening in 400 asymptomatic individuals with increased familial risk. *Radiology*, 195, 35–40, 1995.

[7] R. Simone, I. Wolf, S. Mottl-Link, B. Bottiger, H. Rauch, H. Meinzer and S. Hagl. Intraoperative assessment of right ventricular volume and function. *European Journal of Cardio-thoracic Surgery*, 27, 988–993, 2005.

[8] S.W. Smith. *The Scientists and Engineer's Guide to Digital Signal Processing.* California Technical Pub., San Diego, 1997.

[9] M. Still. *Curve and Surface Fitting: An Introduction.* Academic Press, 2005.

[10] M. Woo, J. Neider and T. Davis. *OpenGL Programming Guide. Second Edition.* Addison-Wesley Pub., Lakewood, 1997.